Microbublle

Physics analysis and modelisation

Measurement data

Medical application

Dr Pierre VANGELUWE

July 2012

Introduction

Advanced medical imaging has a strong impact on research and clinical decision-making. As a matter, real-time imaging assessment of angiogenesis should become a powerfull biomarker in cancer disease (ref irm, us). Ultrasound imaging in B-mode is widely and routinely used owing to the low price per examination and its safety. Those scan shows contrasted regions from transitions in acoustic impedance in the form of brighter pixels. However, blood is a poor scatterer of ultrasound waves at clinical diagnostic transmit frequencies, which lie between 1 and 20 MHz. Then, vascular and perfusion specific imaging tool need markers designed to enhance the contrast. In ultrasound imaging, contrast media consist of microscopically small gas bubbles encapsulated in biodegradable shells.

In this white paper, the physical principles of ultrasound contrast agent microbubble behavior including, US Time frequency analysis up to collapses phase , are analysed and experimentally . Furthermore, an outline of clinical imaging applications of CEUS is given.

1 - Microbublle physics overview

Microbubble distribution analysis

Into medical application, detection strategies have been developed to discriminate acoustic signal-generated by ultrasound contrast agent microbubbles from other acoustic signals such as specular reflections and tissue scattering.

The contrast agent react with flow to produce microbubbles to know the microbubble diameter, we perform a distribution measurement (the serum PHI was mixed with SF6 (sonovue 8 µg/ ml) The distribution measurement is performed :-

The measurement was perform through high speed camera unit, just after the injection

250 gas microbublle are available on the snapshot. For efficiency we choose to rescale all the distribution to 100 microbubble gas unit

Into this measurement, the average diameter Is around 0.5 µm, but with a huge variation (3 factor). A second smapshoot is performed 180 seconds later, Into this second measurement (same picture array) the number of microbublle change (aggregation : now only 190 microbubble) and the max size is 2 um (4 samples) The average diameter is 0.6 µm.

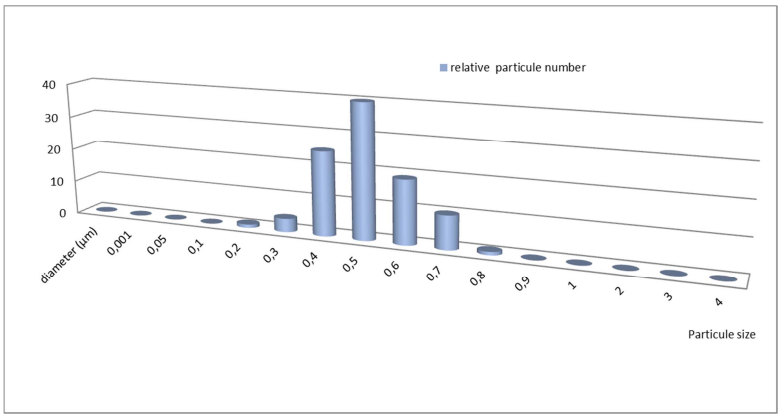

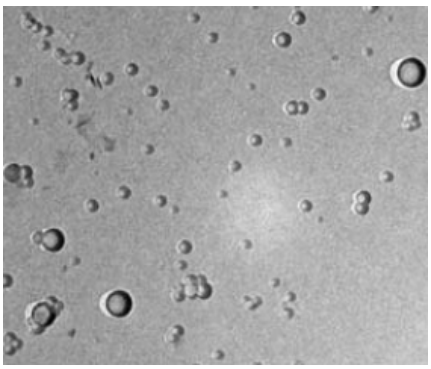

Figure 1: Microbubbles diameter distribution measurement

With this measurement we conclude the diameter distribution is stable on static condition (in vitro during 3 minutes . The max to min ratio is 8. Into the next chapter, we analyze the microbublle variation into a linear pressure variation.

2 - Measurement accuracy impact

Relationship between local pressure and microbbubles diameter:

Blood is a poor scatterer of ultrasound waves at clinical diagnostic transmit frequencies, which lie between 1 and 20 MHz. Since imaging blood flow and measuring organ perfusion are desirable for medical diagnostic purposes, markers should be added to the blood to differentiate between blood and other tissue types.

Physical parameters of microbubbles are adapted to medical application: mean diameter (below 0.4 um to pass through the lung capillaries), type of gas, encapsulating shells made of phospholipids materials. Detailed overviews of the compositions of the ultrasound contrast agents used most in imaging research have been given by Postema et All[3]

The pressure inside a bubble of gas must be higher than the ambient pressure [11]. This difference is generally referred to as the surface pressure and then to the diameter [12]. The smaller the bubble, the higher is the surface pressure. Since fluids are forced to flow from a location with a higher pressure to a location with a lower pressure, a bubble cannot exist in true equilibrium . For example, an oxygen bubble with a 0.4 um diameter dissolves within 14 ms. To prevent quick dissolution, ultrasound contrast agent microbubbles contain low-solubility gas, such as SF6 encapsulation.

Open discussion : (Relation entre Solubilité et pression *?)➔ dans toute l'étude , on suppose que l'on travaille avec une solution homogène . Les problèmes liés entre la solution et la pression sont des épiphénomènes localises pour des pression > 20hP (A priori, cela ne s'applique pas dans notre cas, mais une vérification est indispensable.)*

Influence of ultrasound field characteristics on microbbubles diameter:

On most B-mode ultrasound devices, the intensity of the ultrasonic field is generally adjusted with a mechanical index (MI) instead of the acoustic amplitude. The MI depends on the maximum value of peak negative pressure based into the centrer frequency of the ultrasound field [6]. In commercial scanners, the MI has been limited to 1.9 for medical imaging[8].

We experimentally analyzed SF6 microbbubles diameter variation under different MI. with a network analyser (S parameters measurements (setup measurement and lab test description available into the annexes) All the calculation-simulation were performed with some electronics devices and matlab parameters as close as possible to clinical characteristics. The MI could split into 3 configurations based on clinical knowledge : .. For MI < 0.3, the acoustic amplitude is considered low and not realy useful into this microbublle study.. . Up to MI = 0.7 , which is considered high acoustic amplitude (resonance), clinical risk increases [4].

We focus on MI variation between 0.3 and 0.7 For MI > 0.7, (close to the cavitation process) soft tissue and ultrasound contrast agent including gas microspheres are highlightedInto the lab test we performed measurement up to ML = 0.9, but only to improve the accuracy of curve fitting Fig 2. provides the evolution of the microbubble diameter variation vs MI

Note: This expression could be fitted with the following polynomial function

$$Y = a + b*X+c*\ln(X)+d /X^2$$

a = 0.0235 b = 0.2486 c = 3.4856 d = 5.3254

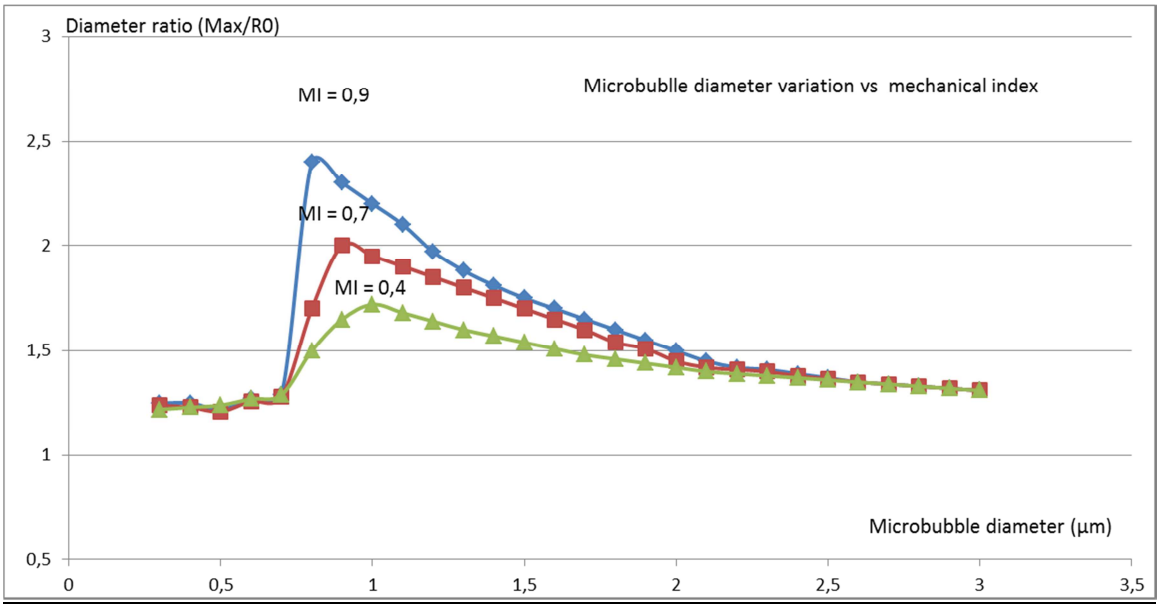

Fig : 2 –Microbubble diameter variation vs MI (tested with acoustic frequency = 5 MHz.

Relationship between microbbubles resonance frequencies and diameter:

For hith accuracy,circulating microbubbles detection, acoustic frequency must correlated with specific resonance frequencies, in the medical ultrasonic range allowing to differentiate from fixed soft tissue. Based on their acoustic properties, microbubbles are well suited as an ultrasound contrast agent. As a matter, the resonance frequencies of encapsulated microbubbles lie slightly higher than those of free gas bubbles[10], but clearly well within the clinical diagnostic range, too.

Experimental measurement of resonance frequencies variations of encapsulated gas microbbubles has been performed through S Parameters (annexe). The setting configuration is shown into the next picture. Agilent E4438 Arbitrary generator generated the pattern, the requested frequency and level. The tektronik TDS 350 is set up to record pattern. Both are time stamped through a RTX technology (real time , high speed clock and synchronization)We generated a constant acoustic field with a vector network analyser. (this system is similar to a close loop system) ML was generated through a dielectric transceiver The ML level is correlated to the voltage swing (sine wave). The receiver was imbedded into the same transceiver.

The two main advantage of this structure are:

- Transmitter and receiver are analyse the same volume.
- Transmitter and receiver impedance are exactly the same (same sensor). By the way this setup is only sensitive into the S11 of the device under test (soft tissues, …) ,

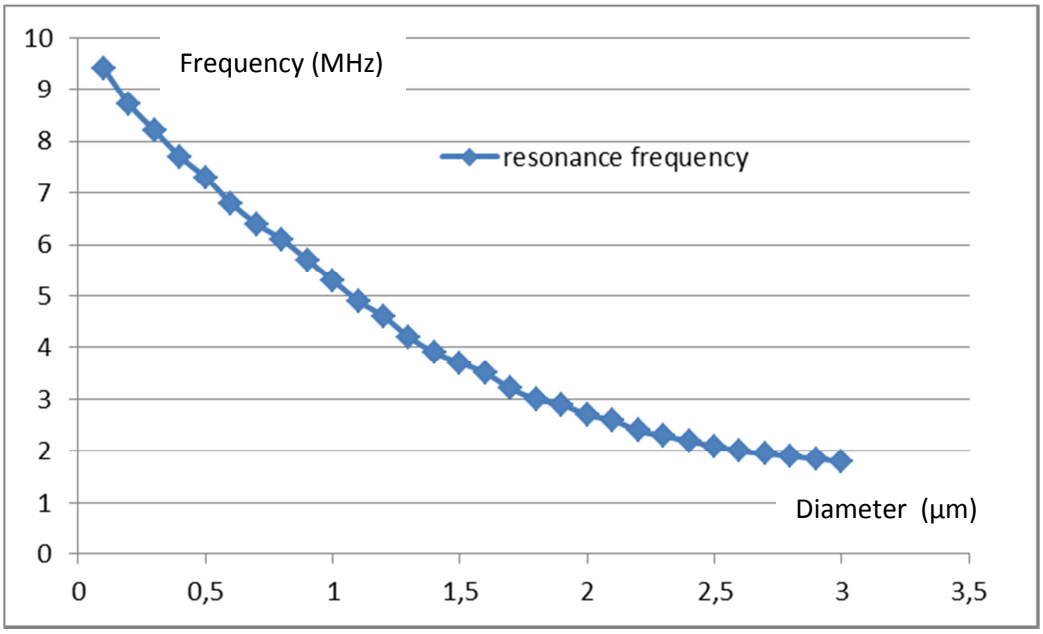

Fig : 3 -Resonance frequency variation vs microbublle diameter

The Figure 3 shows that the resonance frequencies of encapsulated gas microbubbles were a function of their equilibrium radius.

3 – Improvement proposal

We used Scattering parameters to describe the electrical behavior of linear electrical networks (such as acoustic devices) when undergoing various steady state stimuli by acoustic signals.

The parameters are useful to modelize electromagnetic radar devices and could be use for acoustic sub system

Many medical properties of measurement networks (IRM – Oxymeter –Doppler –Acoustic devices) may be expressed using S-parameters, such as gain, return loss, voltage standing wave ratio (VSWR), reflection coefficient and RAW data. Although applicable at any frequency, S-parameters are mostly used for networks operating at Acoustic devices where signal power and energy considerations are more easily quantified than MI. S-parameters change with the measurement frequency, so frequency must be specified for any S-parameter.

First measurement must perform with a 'phantom device ' to determinate the sensitivity of the device. For this test we perform the same echography of the phantom with different ratio ofSF6 into the serum. .

Vascular density evolution.

Setup : The test are performed during some weeks or month. The key target is to estimate the ultrasonic echo variation vs time when microbublle are set .

Each echography test (duration around 180 seconds.) could estimate through RAW data and Vidéo for ROI (manual aera estimation) , or video data and RO (same procedure)

Into this procedure, the main key issues are

- The unknown of the echography unit noise level (Raw data measurement)
- The unknown of the echography unit (video Bandwith (Video data degradation vs Raw Data)
- Accuracy of the ROI (user discrimination) : Raw data variation

- On contrast enhanced ultrasound, the intensity of the ultrasonic field displayed is related to the microbubble frequency response (resonance) , by the way, the diameter distribution impact the measured enhancement of the tissues .

measurements stated, in addition to the characteristic impedance or system impedance.

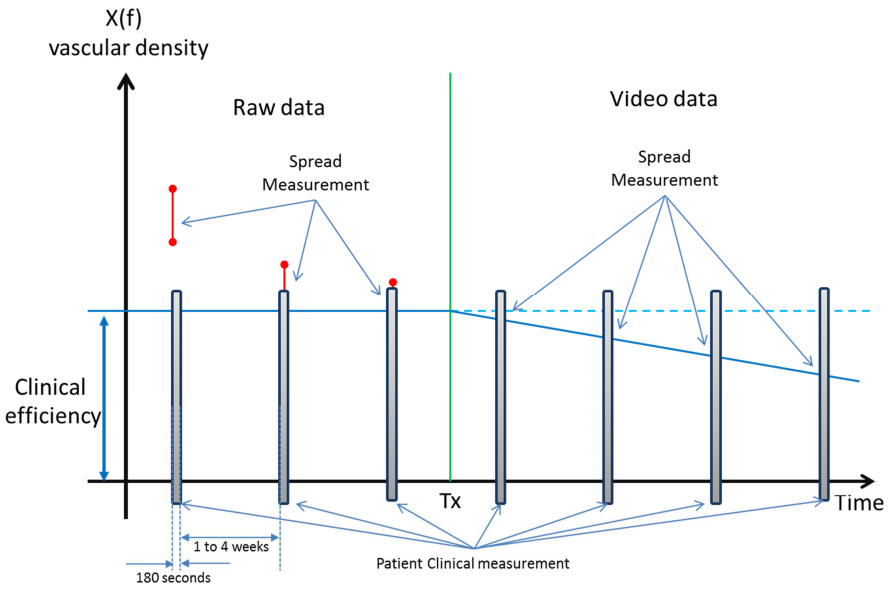

Automatic ROI detection proposal

Due to those previous unknown, we propose to estimate the spread variation correlated to tumor variation base on manual ROI decision. We propose to replace manual ROI with automatic ROI selection

The region of interest is a particular region in a scene in which we are interested..
Therefore, it is essential to extract that region from the scene which has significant information. In order to extract significant region there need to determine its cognitive boundary.
In this proposal, we treat this boundary as ROI. The selection of this cognitive boundary by human itself is difficult. This is because humans have different psychology of interest and decision making criteria.Then how will we define such boundary autonomously What things are to be included and what things are to be excluded from this boundary.. In the case of visual scene, human tries to observe the interesting objects in the scene. This needs selection of ROI which confines objects of interest in it. Relevance theory claims that humans do have an automatic tendency to maximize relevance, not because we have a choice in the matter Automatic video ROI determination is described into the next paragraph,, ranking algorithm in and automatic detection and tracking of salient objects

Into this architecture proposal , we use a matrix of 256 elements. (each line or colon avec a subdivision of 64 pixels (or Raw data) as shown into the next figure

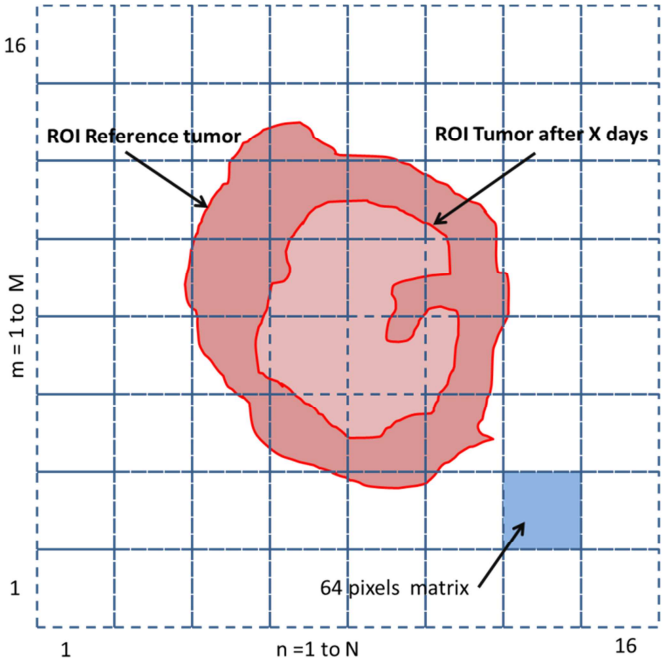

Fig. 5…Representative tumor estimation between two separate analysis on sub matrix representation.

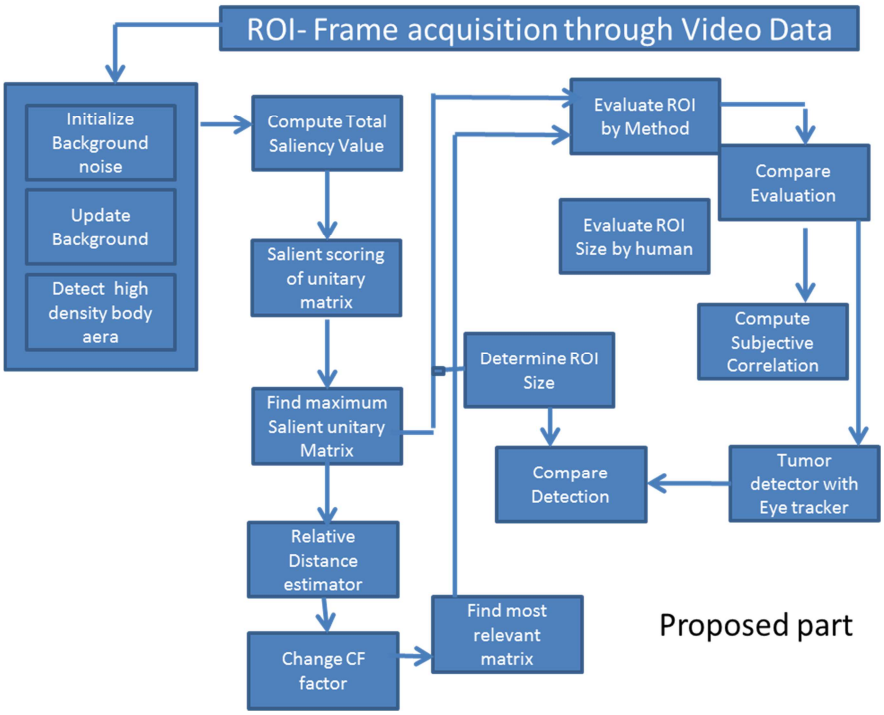

For example, with this previous structure, we post process the ROI available on IGR structure. This post processing will provide without manual ROI manual design, rehausment curve on each sub matrix . Into the next figure, we provide a rehausment fitting curve for each sub matrix. The average rehausment curve is the the sum of significant rehausment curve divide by the munmber of significant sub matrix. The treat hold ..of signifant/no significant rehausment curve isvalidate if the peak to average is up to SQR(2). After the following structure, we display a 3D curve representative of the rehausment curve vs time. This display should useful and it's a break through analysis.

Receiver acoustic wave, processed with a real time DSP Texas Instruments (6 G flops). This strategy achieve a 300000 samples FFT for each frame. The frequency and the amplitude of each peak between 1 MHz to 40 MHz show into the figure 5 is representative to the microbubbles diameter distribution.

Medical protocol:

For the existing configuration and the new proposal protocol, the medical setup is similar.

Existing protocol

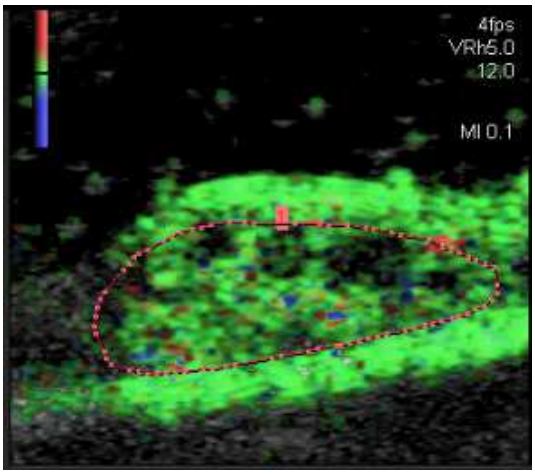

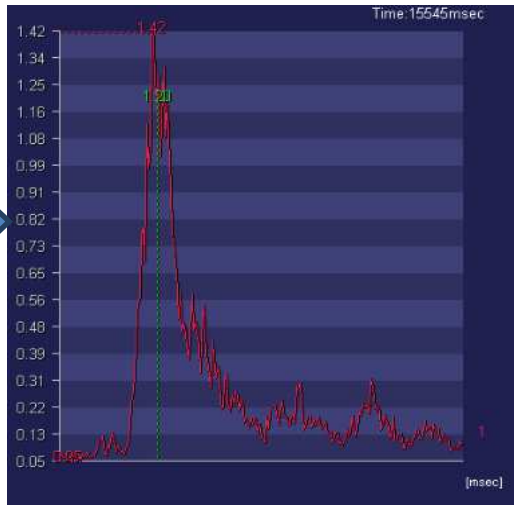

Image vidéo data - time : t = 15545 mS
Courbe rouge ROI IGR

<u>Avantages:</u>

-ROI simple à dessiner

<u>Limitations</u>

- Determination manuelle de la ROI.
- Courbe de réhaussement fortement perturbé (lié à la variation de la sonde/opérateur)
- ROI dépend de l'opérateur
- Temps pour la saisie (pour ROI complexes)
- Sensibilité dégradée si existance de zone échogène non uniforme.
- Pas de synchronisation /mouvement de la sonde
- Pas de discrimination de zones.
- Visualisation 3D impossible

Proposal protocol

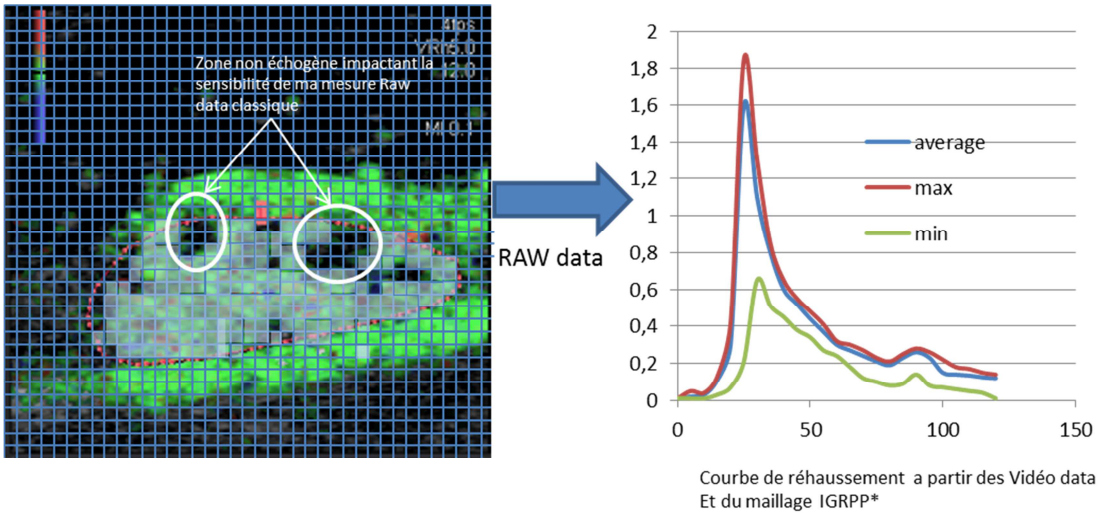

Avantages:

- Aucune ROI a dessiner.
- Discrimination automatique de zones inta-tumorales (nécroses)
- Amélioration de la précision moyenne
- Information sur la surface/volume tumoral pour chaque examen
- Courbe de réhaussement Min et Max

automatiquement générées.

- Synchronisation de l'image avec les mouvements de la sonde.
- Visualisation 3D de la courbe de réhaussement.
- Algorithme supporte les imageurs 3D

- **Limitations**

- Temps de processing (2H pour 180 secondes d'enregistrement a 4fps)
- La zone de la tumeur ne doit pas depasser 74 % de la zone d'acquisition.

Développement 3D non validé

Conclusion

It is a challenging task to quantify and predict which bubble phenomenon occurs under which acoustic condition, and how these may be utilized in ultrasonic imaging. Aided by Time Frequency measurement (TDMA burst) , we can improve understanding of encapsulated microbubble behavior reability More sophisticated medical methods use quantitative approaches to measure the amount and the time course of bolus or reperfusion curves and have shown great promise in revealing an effective tumor response to anti-angiogenic drugs in humans before tumor shrinkage occurs.

y a eu deux methodes : visuelle (video data) en 2D qui est efficace dans certains cas; et la deuxieme avec les raw data qui pretend mesurer le signal a partir de courbes mais qui n'est pas prouvée.

A MON AVIS: il existe un seuil de densité vasculaire et de parameters hémodynamiques a partir duquel cette technique (quantification par DCEUS) peut apporter des infos reproductibles. Cad a dire a partir d'un certain degre de necrose (desertification vasculaire) les video data sont utiles.

SOUS ce seuil, les données (meme raw data) sont trop « imprecises » pour les raisons physiques decrite ci dessus

In conclusion, combining ultrasound contrast agents with TDMA Time Frequency analysis lead to simple and economic methods, using conventional ultrasound scanners with accuracy improvement

REFERENCES

Lassau N, Lamuraglia M, Chami L, Leclère J, Bonvalot S, Terrier P, Roche A, Le Cesne A. Gastrointestinal stromal tumors treated with imatinib: monitoring response with contrast-enhanced sonography. AJR Am J Roentgenol 2006; 187: 1267-1273

Magnon C, Galaup A, Rouffiac V, Opolon P, Connault E, Rosé M, Perricaudet M, Roche A, Germain S, Griscelli F, Lassau N. Dynamic assessment of antiangiogenic therapy by monitoring both tumoral vascularization and tissue degeneration. Gene Ther 2007; 14: 108-117

Postema M. Bubbles and ultrasound. Appl Acoust 2009; 70: 1305

ter Haar G. Safety and bio-effects of ultrasound contrast agents. Med Biol Eng Comput 2009; 47: 893-900

Postema M, Schmitz G. Bubble dynamics involved in ultrasonic imaging. Expert Rev Mol Diagn 2006; 6: 493-502

Webb A. Introduction to Biomedical Imaging. Hoboken: John Wiley and Sons, 2003

Wells PNT. Ultrasonic imaging of the human body. Rep Prog Phys 1999; 62: 671-722

British Medical Ultrasound Society. Guidelines for the safe use of diagnostic ultrasound equipment. Ultrasound 2010; 18: 52-59

Postema M, Gilja OH. Ultrasound-directed drug delivery. Curr Pharm Biotechnol 2007; 8: 355-361

Voigt JU. Ultrasound molecular imaging. Methods 2009; 48: 92-97

Schmitz G. Ultrasound in medical diagnosis. In: Pike R, Sabatier P, editors. Scattering: scattering and inverse scattering in pure and applied science. London: Academic Press, 2002: 162-174

Macdonald CA, Sboros V, Gomatam J, Pye SD, Moran CM, Norman McDicken W. A numerical investigation of the resonance of gas-filled microbubbles: resonance dependence on acoustic pressure amplitude. Ultrasonics 2004; 43: 113-122

Guan J, Matula TJ. Using light scattering to measure the response of individual ultrasound contrast microbubbles subjected to pulsed ultrasound in vitro. J Acoust Soc Am 2004; 116: 2832-2842

Postema M. Fundamentals of medical ultrasonics. London: Spon Press, 2011

Postema M, Bouakaz A, de Jong N. Noninvasive microbubble-based pressure measurements: a simulation study. Ultrasonics 2004; 42: 759-762

Schutt EG, Klein DH, Mattrey RM, Riess JG. Injectable microbubbles as contrast agents for diagnostic ultrasound imaging: the key role of perfluorochemicals. Angew Chem Int Ed Engl 2003; 42: 3218-3235

Wrenn SP, Mleczko M, Schmitz G. Phospholipid-stabilized microbubbles: Influence of shell chemistry on cavitation threshold and binding to giant uni-lamellar vesicles. Appl Acoust 2009; 70: 1313-1322

Sboros V. Response of contrast agents to ultrasound. Adv Drug Deliv Rev 2008; 60: 1117-1136

Lassau N, Lamuraglia M, Koscielny S, Spatz A, Roche A, Leclere J, Avril MF. Prognostic value of angiogenesis evaluated with high-frequency and colour Doppler sonography for preoperative assessment of primary cutaneous melanomas: correlation with recurrence after a 5 year follow-up period. Cancer Imaging 2006; 6: 24-29

Cosgrove D, Lassau N. [Assessment of tumour angiogenesis using contrast-enhanced ultrasound]. J Radiol 2009; 90: 156-164

Lassau N, Koscielny S, Albiges L, Chami L, Benatsou B, Chebil M, Roche A, Escudier BJ. Metastatic renal cell carcinoma treated with sunitinib: early evaluation of treatment response using dynamic contrast-enhanced ultrasonography. Clin Cancer Res 2010; 16: 1216-1225

Annexes:

The S-parameter matrix applied to the microbubble acoustic model

For a acoustic cf network, each of the ports is ranging from 1 to 2, , the associated S-parameter definition is in terms of incident and reflected 'power waves', a_n and b_n respectively.

Kurokawa[7] defines the incident power wave for each port as

$$a = \frac{1}{2}k(V + Z_p I)$$

and the reflected wave for each port is defined as

$$b = \frac{1}{2}k(V - Z_p^* I)$$

where Z_P is the diagonal matrix of the complex reference impedance for each port, Z_P^* is the element wise complex conjugate of Z_P

$$k = \left(\sqrt{|\Re\{Z_p\}|}\right)^{-1}$$

Sometimes it is useful to assume that the reference impedance is the same for all ports in which case the definitions of the incident and reflected waves may be simplified to

$$a = \frac{1}{2}\frac{(V + Z_0 I)}{\sqrt{|\Re\{Z_0\}|}} \quad \text{and} \quad b = \frac{1}{2}\frac{(V - Z_0^* I)}{\sqrt{|\Re\{Z_0\}|}}$$

For all ports the reflected power waves may be defined in terms of the S-parameter matrix and the incident power waves by the following matrix equation:

$$b = Sa$$

Lossy networks : patient modelisation

Medical acoustic solution should modelize with S parameters as a lossy passive network. Into those solution, one in which the sum of the incident powers at all ports is greater than the sum of the reflected powers at all ports. It therefore dissipates power, or : $\Sigma|a_n|^2 \neq \Sigma|b_n|^2$. In this case $\Sigma|a_n|^2 > \Sigma|b_n|^2$, and $(I) - (S)^H(S)$ is positive definite.

Two-Port S-Parameters

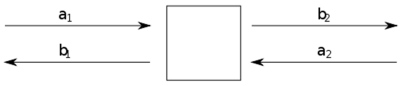

The medical acoustic S-parameter matrix for the 2-port network. The relationship between the reflected, incident power waves and the S-parameter matrix is given by:

$$\begin{pmatrix} b_1 \\ b_2 \end{pmatrix} = \begin{pmatrix} S_{11} & S_{12} \\ S_{21} & S_{22} \end{pmatrix} \begin{pmatrix} a_1 \\ a_2 \end{pmatrix}$$

Expanding the matrices into equations gives:

$$b_1 = S_{11}a_1 + S_{12}a_2 \quad \text{and} \quad b_2 = S_{21}a_1 + S_{22}a_2$$

Each equation gives the relationship between the reflected and incident power waves at each of the network ports, 1 and 2, in terms of the network's individual S-parameters, S_{11}, S_{12}, $S_{21}$and S_{22}. If one considers an incident power wave at port 1 (a_1) there may result from it waves exiting from either port 1 itself (b_1) or port 2 (b_2). However if, according to the definition of S-parameters, port 2 is terminated in a load identical to the system impedance (Z_0) then, by the maximum power transfer theorem, $b_2$will be totally absorbed making $a_2$equal to zero. Therefore

$$S_{11} = \frac{b_1}{a_1} = \frac{V_1^-}{V_1^+} \quad \text{and} \quad S_{21} = \frac{b_2}{a_1} = \frac{V_2^-}{V_1^+}$$

Acoustic logarithmic gain

The scalar logarithmic (decibel or dB) expression for gain (g) is

$$g = 20\log_{10}|S_{21}|_{\text{dB}}.$$

This is more commonly used than scalar linear gain and a positive quantity is normally understood as simply a 'gain'... A negative quantity can be expressed as a 'negative gain' or more usually as a 'loss' equivalent to its magnitude in dB. For example, a 1 cm of skin may have a gain of - 4 dB at 3.5 MHz or a loss of 4 dB at 3.5 MHz.

Insertion loss

In case the two measurement ports use the same reference impedance, the insertion loss (IL) is the dB expression of the transmission coefficient $|S_{21}|$. It is thus given by:[10]

$$IL = -20\log_{10}|S_{21}|_{\text{dB}}.$$

It is the extra loss produced by the introduction of the DUT between the 2 reference planes of the measurement. Notice that the extra loss can be introduced by intrinsic loss in the DUT and/or mismatch. In case of extra loss the insertion loss is defined to be positive.

Input / Output return loss

Input and Output return loss ($RL_{\text{in}}RL_{\text{out}}$) is a scalar measure of how close the actual input impedance of the network is to the nominal system impedance value and, expressed in logarithmic magnitude, is given by

$$RL_{\text{in}} = |20\log_{10}|S_{11}||_{\text{dB}}. \qquad RL_{\text{out}} = |20\log_{10}|S_{22}||\ \text{dB}.$$

Reverse gain and reverse isolation

The scalar logarithmic (decibel or dB) expression for reverse gain (g_{rev}) is:

$$g_{\text{rev}} = 20\log_{10}|S_{12}|_{\text{dB}}.$$

Often this will be expressed as reverse isolation (I_{rev}) in which case it becomes a positive quantity equal to the magnitude of $g_{\text{rev}}$and the expression becomes:

$$I_{\text{rev}} = |g_{\text{rev}}| = |20\log_{10}|S_{12}||_{\text{dB}}.$$

This reverse gain is extremely sensitive to the impedance variation (correlated to the impedance variation due to microbubble variation.

Acoustic standing wave ratio

The acoustic standing wave ratio (ASWR) at a port, represented by the lower case 's', is a similar measure of port match to return loss but is a scalar linear quantity, the ratio of the standing wave maximum MI to the standing wave minimum power. It therefore relates to the magnitude of the MI reflection coefficient and hence to the magnitude of either $S_{11}$for the input port or $S_{22}$for the output port.

At the input port, the VSWR ($s_{\mathbf{in}}$) is given by $s_{\mathrm{in}} = \frac{1 + |S_{11}|}{1 - |S_{11}|}$

At the output port, the VSWR ($s_{\mathbf{out}}$) is : $s_{\mathrm{out}} = \frac{1 + |S_{22}|}{1 - |S_{22}|}$

The RF Toolbox add-on to MATLAB[16] use this last definition to estimate the power distribution vs microbubble diameter variation.

Calibration

For, it is mandatory to perform specific calibration .Prior to making a tumor estimation including S-parameter measurement, the first essential step is to perform an accurate calibration appropriate to the intended measurements. Several types of calibration are identity. The calibration needs advanced processing capability, at realistic accuracy including corrections for systematic errors.[19] The more basic types, often called 'response' calibrations, may be performed quickly but will only provide a result with moderate uncertainty. For improved uncertainty and dynamic range of the measurement a full 2 port calibration is required prior to DUT measurement. This will effectively eliminate all sources of systematic errors inherent in the accoustic measurement system.

Minimization of systematic errors

Systematic errors are those which do not vary with time during a calibration. For a set of 2 port S-parameter measurements there are a total of 12 types of systematic errors which are measured and removed mathematically as part of the full 2 port calibration procedure. They are, for each port:

1. directivity and crosstalk
2. source and load mismatches
3. frequency response errors caused by reflection and transmission tracking within the test receivers

The calibration procedure requires initially setting up the test:

with all the medical requested configuration (, Frequency , Probes, MI, …). A calibration prodedure is used according to the microbublle diameter.

Even with configuration of high quality, when performing tests at the higher frequencies ivarious stray materials will become apparent and cause uncertainty during the calibration. Data relating to the strays of the particular calibration unit

The calibration procedure could software controlled, and instructs the operator to fit various configuraition

At each step the VNA processor captures data across the test frequency range and stores it. At the end of the calibration procedure, the processor uses the stored data thus obtained to apply the systematic error corrections to all subsequent measurements made. All subsequent measurements are known as 'corrected measurements. At this point the raw data processing tools are able to corrected measurement through S-parameters.

Hardware setup

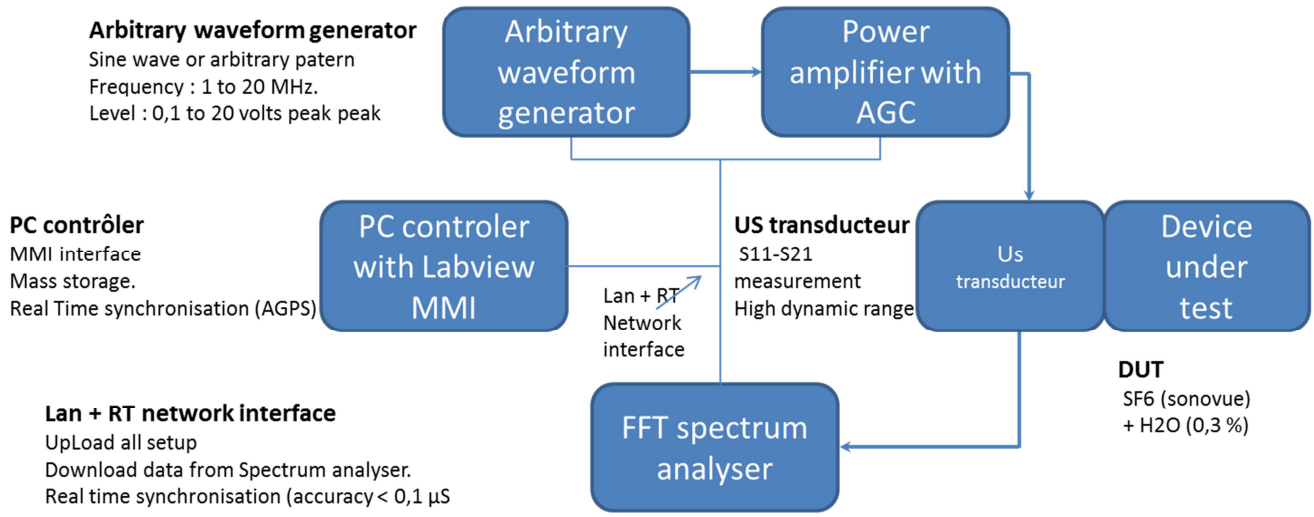

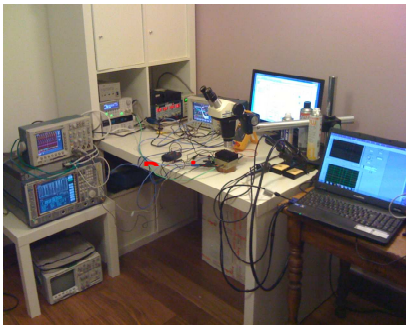

FFT Spectrum Analyser
Real time S11 and S21 measurement
Wide range analysis (10 MHz span – 10 kHz RBW – 10 kHz VBW).
Deep log detection (dynamic range : 135 dB noise level : -120 dBm)

S21 transceiver gain (reference to 0 dB)